

# Image Cover Sheet

**CLASSIFICATION**

**SYSTEM NUMBER**

510371

UNCLASSIFIED



**TITLE**

DIFFRACTION MEASUREMENTS ON CPF STEEL FATIGUE SAMPLES

**System Number:**

**Patron Number:**

**Requester:**

**Notes:** Paper #28 contained in Parent Sysnum #510343

**DSIS Use only:**

**Deliver to:** DK



## Diffraction Measurements on CPF Steel Fatigue Samples

by

Percy Clark\*, Tom Holden\*, John F. Porter\*\* and Richard Yee\*\*\*

\* Atomic Energy of Canada Limited, Chalk River Laboratories,  
Chalk River, Ontario, Canada, NOR 1L0

\*\* Defence Research Establishment Atlantic, Dockyard Lab,  
FMO Halifax, Halifax, Nova Scotia, Canada, B3K 2X0

\*\*\* Fleet Technology Limited, Kanata, Ontario, Canada, K2K 1Z8

### ABSTRACT

In an effort to develop a non-destructive means of quantifying fatigue damage in cyclically loaded marine materials, prior to the formation of a detectable fatigue crack, a series of hourglass shaped specimens were fabricated from 350WT steel, cyclically loaded to various percentages of their fatigue crack initiation life, and examined via neutron diffraction methods. Diffraction line parameters were observed which varied strongly with distance from the waist of each specimen. These parameters correlated with the degree of induced fatigue damage. Comparisons were made between these experiments and earlier less successful similar experiments conducted on HY80 samples. The limitations and potential for the application of diffraction technologies to non-destructively define the remaining fatigue life in marine components and structures is reviewed.

## 1.0 INTRODUCTION

Diffraction techniques are possible non-destructive methods of evaluating plastic deformation or fatigue damage in marine components which have been subjected to cyclic loading. This makes them attractive for assessing remaining fatigue life in naval vessels.

Several workers have tried to assess the accumulation of fatigue damage by monitoring the changes in residual stress and line broadening with fatigue life using x-rays. Both Goto<sup>1</sup> who studied fatigued 17-4 PH steel and Pangborn *et al*<sup>2</sup> who studied aluminum alloys found that line broadening was more sensitive to 'fatigue damage' in the first and last 10% of fatigue life. Pangborn *et al* suggested that 'fatigue damage' was accumulated in the interior of the specimen and recommended the use of more penetrating Mo  $k_{\alpha}$  x-rays to study this possibility. For steel specimens, sufficient penetration can only be achieved by employing neutron scattering techniques.

To study the behaviour of residual strains and line broadening in fatigued CPF steels and to test the feasibility of predicting remaining fatigue life using neutron diffraction, samples of CPF steel were fatigue tested by Fleet Technology Ltd. under varying stress ranges and these samples were then examined using neutron diffraction techniques at Chalk River Laboratories.

### 1.1 Line Broadening Measurements

A peak measured in a diffraction experiment using a perfectly collimated, zero wavelength spread instrumental set-up and a large, defect free diffracting crystal has the general form of a near delta-function due to the coherently scattered radiation superimposed on a slowly varying background. The width of the sharp coherent component has a predicted full width at half intensity (FWHM) of 7.61 arcseconds<sup>3</sup>, called the Darwin width.

If the crystal is plastically deformed, the generation of dislocations broadens the diffraction peak through two mechanisms. The dislocations allow a non-uniform strain field to exist within the crystal which introduces a Gaussian component to the lineshape. With sufficient deformation, the dislocations can form tangled walls that break up the coherently scattering crystal into small sub-grains. This produces a particle size broadening effect, giving rise to a Lorentzian component to the lineshape. It is possible to separate the two effects by Fourier analysis

using careful measurements of the lineshape for multiple peaks over a range of diffraction angles (Warren-Averbach analysis)<sup>3</sup>. For the purpose of the current work a simpler and more direct approach was preferred.

Kurita and Chiaki<sup>4</sup> used the FWHM ( $\Delta_o$ ) obtained from a Gaussian fit to a single diffraction peak in an attempt to assess plasticity in mild steels. They found that the linewidth varied linearly with the logarithm of the plastic strain ( $\epsilon$ ) according to the form

$$\epsilon = A \times 10^{C\Delta_o} \quad (1)$$

Where  $A$  and  $C$  are empirical constants. This approach is reasonable, in this case, since both the non-uniform strain and particle size effects are the result of dislocation based plastic deformation; the parameter of interest.

In any real diffraction experiment, the spread of radiation wavelength and the finite angular collimations of the incident and scattered beams contribute to an additional instrumental linewidth  $\Delta_I$ . From a measurement of the linewidth of a well annealed reference nickel powder with negligible deformation broadening,  $\Delta_I$  can be determined. The intrinsic deformation linewidth ( $\Delta$ ) can be found by subtracting the instrumental linewidth from the observed linewidth ( $\Delta_o$ ) in quadrature as follows

$$\Delta^2 = \Delta_o^2 - \Delta_I^2 \quad (2)$$

## 2.0 EXPERIMENTAL

### 2.1 Samples

Fleet Technology Ltd. fatigue tested 11 standard hourglass specimens of 350WT CPF steel at various stress ranges to determine an approximate S-N curve. Samples 1 and 3 were tested at low stresses and did not fail, while samples 2, 4-11 were tested to failure. The samples were tested at a stress ratio of 0.05. Samples 2-11 were shipped to Chalk River for neutron diffraction analysis. An additional set of 6 samples (A-F) were subjected to a varying number of cycles at various stress ranges. These unbroken samples were sent to Chalk River 'blind', that is, with unknown stress ranges and numbers of cycles to investigate the possibility of determining remaining fatigue life from diffraction measurements.

## 2.2 Neutron Diffraction

The experiments were carried out at the NRU reactor, Chalk River. The L3 spectrometer was used in a high resolution configuration, with the (331) planes of a Germanium monochromator selecting neutrons of wavelength  $1.9895\text{\AA}$  at a take-off angle,  $2\theta_m=100^\circ$ . The angular collimations between the monochromator and sample, and the sample and the detector were  $0.16^\circ$  and  $0.125^\circ$  respectively. Accurate linewidth measurements require high statistical definition of the peak and typically the peak intensity was about 5000 counts. The wavelength of the neutron beam was calibrated with a standard Ni powder. The (111) powder peak of Ni is very close in scattering angle to the (110) iron reflection and the former gives a measure of the instrumental contribution to the linewidth of  $0.256\pm 0.003^\circ$ . The lattice parameter used in the calculation of lattice strain was determined from an untested fatigue specimen and was found to be  $2.0270\pm 0.0001\text{\AA}$ .

The incident and diffracted neutron beams were spatially defined by slits placed in neutron absorbing cadmium. The intersection of the two beams defines the region from which the diffraction information is obtained, the gauge volume. In this case, the gauge volume was approximately cubical, 1.5mm on a side. By placing the samples on a computer controlled xyz stage the location of the gauge volume could be arbitrarily positioned in the sample. The diffraction peak was measured using a position sensitive detector and recorded in the form of intensity versus diffraction angle,  $2\theta$ . The peak position,  $2\theta_{hkl}$ , the integrated intensity,  $I_{hkl}$ , and the line width,  $\Delta_\theta$ , were obtained by fitting a Gaussian distribution plus a sloping background to the data.

For each of the samples tested to failure (samples 2, 4-11), one remnant was measured at five axial positions: 2, 4, 6, 8 and 10mm from the break. The samples fatigued to a fixed number of cycles before failure (samples 3, A-F) were measured at the waist and 5mm above and below.

## 3.0 RESULTS

### 3.1 Fatigue Testing

The results of fatigue testing on samples 1-11 by Fleet Technology Ltd. is shown in Table I. It was determined that the fatigue life ( $N$ ) could be represented by the following function of the stress range ( $S$ ) in MPa

$$\log(N) = 118.3 - 42.18 \log(S) \quad (3)$$

The diameter of the samples was measured as a function of axial position after testing. Using the measured starting diameters of the specimens, the true macro-strain was calculated as a function of axial position and is shown in figure 1 for each of the broken samples.

Specimen Number	Stress Range (MPa)	Life Cycles
1	422	>3.8 million
3	446	>7 million
5,8	455	327 770, 289 320
4,11	485,484	208 490, 114 890
2,10	496, 498	46 410, 40190
9	506	2 870

**Table I** Specimens Tested to Establish the S-N Curve

### 3.2 Neutron Diffraction

Figure 2 shows the results of the diffraction measurements on the broken samples as a function of axial position. Both the line width ( $\Delta$ ), after correction for instrumental broadening, and the residual lattice strains were fit with a linear function of the axial position. From the linear fits the lattice strain and line broadening were calculated at the 0mm and 5mm positions and show a rough linear behaviour when plotted against the fatigue stress range as shown in figures 3 and 4.

The results of the broadening and lattice strain measurements at the waist position for the 6 'blind' samples are plotted in figures 5 and 6 as a function of the true macro-strain derived from diameter measurements before and after testing.

#### 4.0 ANALYSIS

From the calculated macro-strain as a function of axial position and the linear fits of  $\Delta$  versus sample position it was possible to infer the variation of  $\Delta$  with true macro-strain for each sample as shown in figure 7. This was done to separate the role of fatigue damage from the effect of the considerable plastic deformation due to necking that can be seen in figure 1.

Inspection of figure 7 indicates that the data from all the broken samples lies on a single curve that is well described by a logarithmic relationship between macro-strain and the instrumental corrected broadening

$$\Delta = (0.071 \pm 0.001) \times \ln(\epsilon) + 0.322 \pm 0.002 \quad (4)$$

This Kurita-Chiaki behaviour indicates that the broadening behaviour is dominated by the overall plastic deformation and that the number of cycles or remaining fatigue life may have little impact. That is, if the broadening were dominated by remaining fatigue life, samples tested at lower stress ranges and failing at lower macro-strains should deviate from the overall curve of the samples failing at high cycles. For example, if fatigue damage was a significant component of the observed broadening, the terminal broadening of samples 5 and 8 at  $\epsilon=0.35$  and  $\epsilon=0.73$ , respectively, should be much higher than the broadening of samples 2, 10 and 11 (which have much larger remaining fatigue life and a lower number of cycles at the corresponding strains and axial positions). This is not a surprising result given the large degree of plastic deformation due to necking apparent in figure 1.

A similar approach was used to derive figure 8, which relates the measured residual lattice strain as a function of  $\epsilon$ . Clearly, the data from the different samples do not follow a single master curve as closely as in figure 7. However, this is due to the relatively larger error of the lattice strain measurement. The data from all the samples actually do agree within the estimated error. Figure 9 shows the results of plotting the lattice strain along two constant  $\epsilon$  slices through the data in figure 8. There is a large scatter and the slopes are on the order of the uncertainty. As well, following the argument in the previous paragraph, fatigue damage-induced broadening should yield a negative slope in figure 9. That the slope is actually positive is further evidence that the fatigue damage is completely swamped by the necking-induced plastic deformation.

Accepting it is the gross plastic deformation that dominates the broadening and lattice strain behaviour, the increasing  $\Delta$  and increasing compressive lattice strain



with increasing stress range seen in figures 3 and 4 is understandable. Since the samples tested at high stress ranges failed after fewer cycles and therefore in a more ductile failure mode, the macro-strains at the 0 and 5mm positions away from the break were higher.

In both figures 7 and 8 the data from the seven unbroken samples were also plotted and agree well with the overall behaviour of the broken samples.

## 5.0 CONCLUSIONS

Line broadening and lattice strain measured using neutron diffraction in CPF steels fatigue tested to failure are both sensitive indicators of the total plastic strain to which the material has been subjected. The line broadening was found to follow a logarithmic function of the plastic strain as reported by Churita and Chiaki<sup>5</sup>. However, it was found that neutron scattering measurements on samples cycled to failure did not provide indication of fatigue damage. Therefore, it was not possible to predict the remaining fatigue life in the 'blind', unbroken samples.

There are several possible reasons why the measurements reported here were insensitive to fatigue history. Since the samples were measured after failure, it was not possible to make measurements exactly at the waist. As well, it is possible that any effect of the fatigue damage was erased by plastic flow during the final ductile necking failure. The effect of the ductile necking was enhanced since the samples investigated had been tested in the low-cycle fatigue regime. Therefore, more experiments should be performed before and after failure on samples tested at lower nominal stress ranges where failure is expected at lower plastic strains.

## 6.0 REFERENCES

1. Goto, T., "Material Strength Evaluation and Damage Detection by X-ray Diffraction", in Advances in X-ray Analysis, v35, 1992, pp 489-501.1.
2. Pangborn, R.N., et. al, "Dislocation Distribution and Prediction of Fatigue Damage", Met. Trans A, V12A, Jan. 1981, pp 109-120.
3. B.E. Warren, X-Ray Diffraction, Addison Wesley : Reading Mass. (1969).
4. M. Kurita and K. Chiaki, Advances in X-ray Analysis, ed. by C.S. Barrett, Plenum Press: New York 34, 633 (1991)

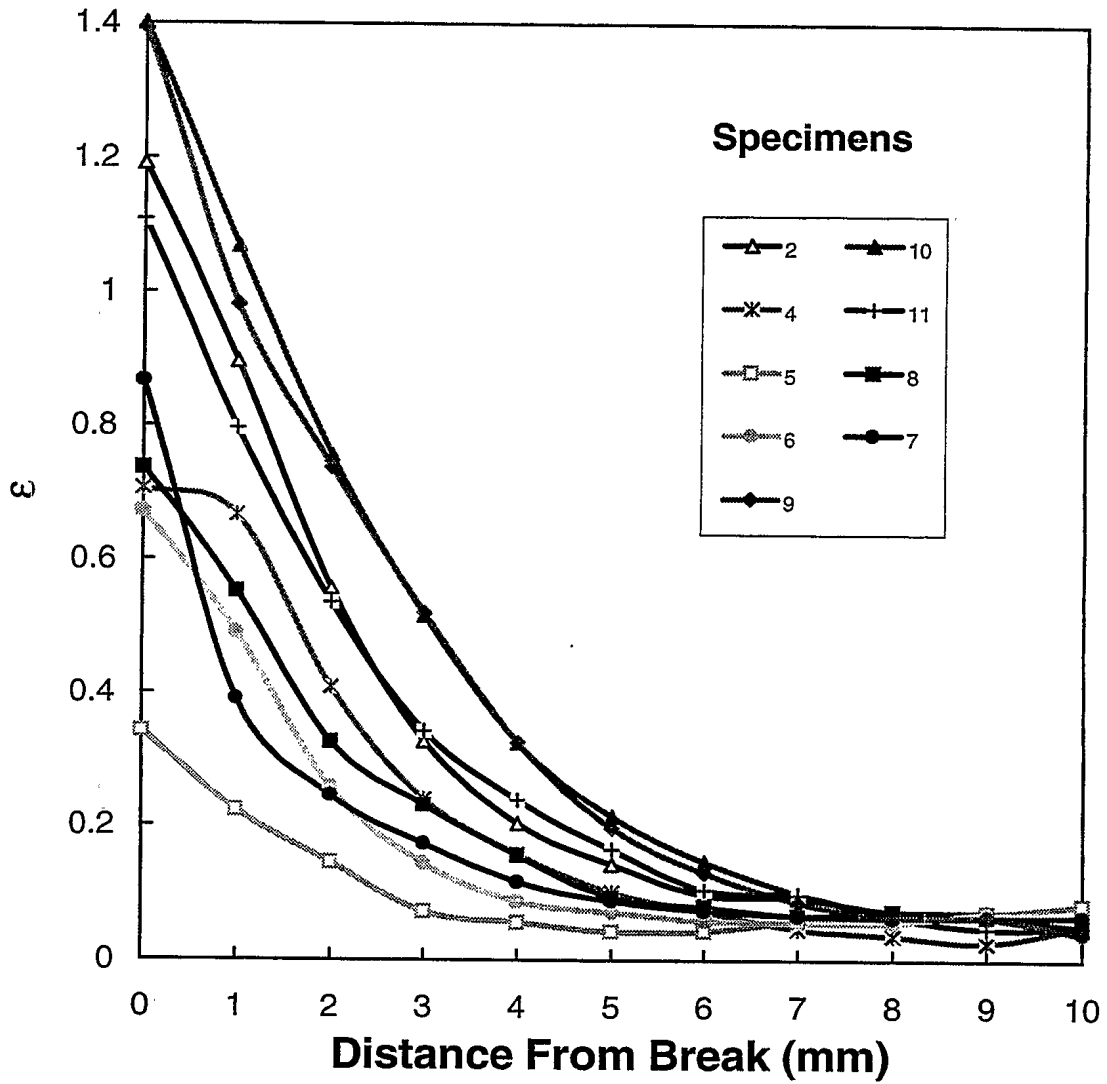


Figure 1 True plastic strain as a function of axial position away from the break for nine samples cycled to failure.

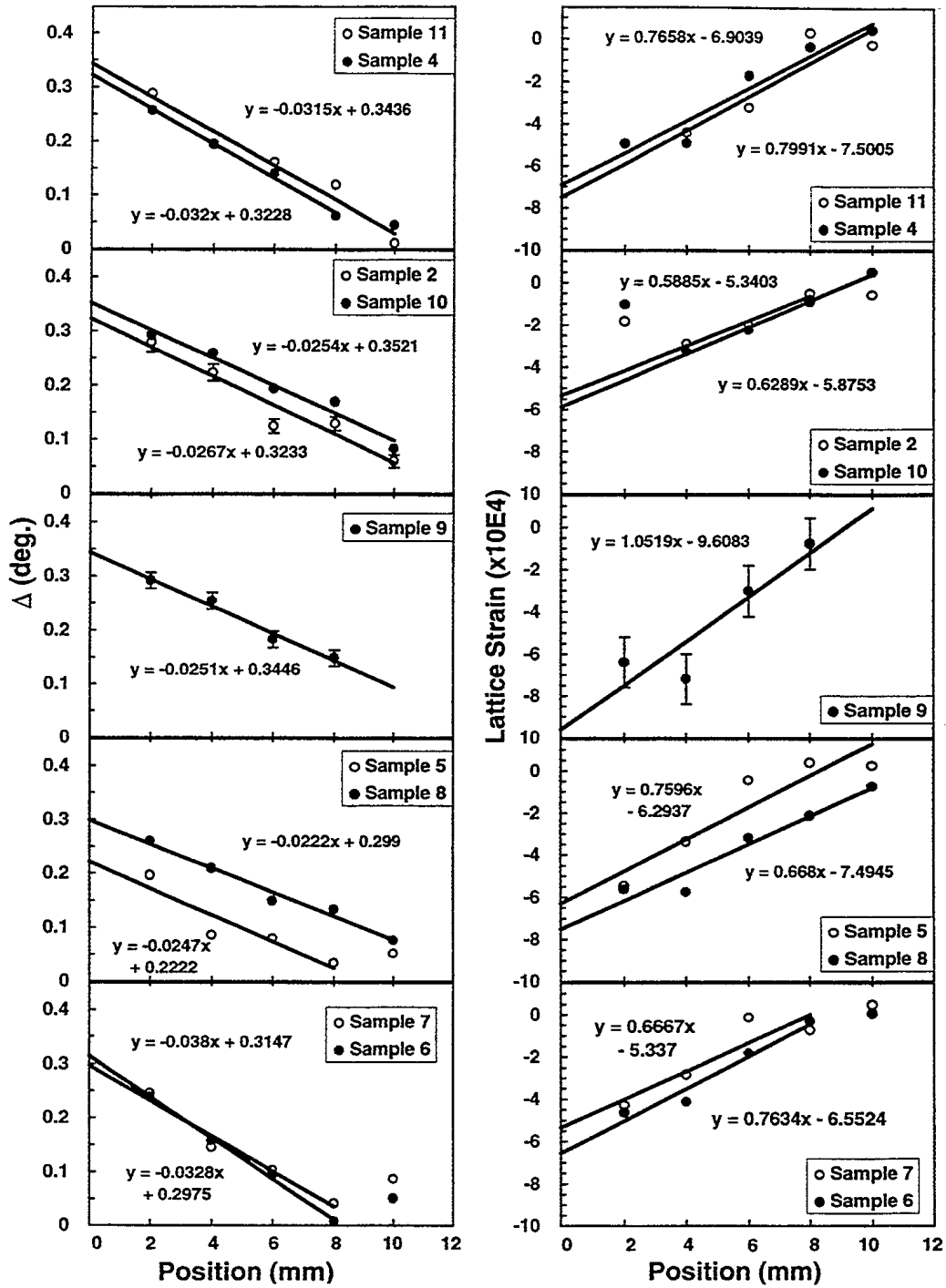


Figure 2 The (110) diffraction linewidth corrected for instrumental broadening and residual lattice strain for nine samples cycled to failure.

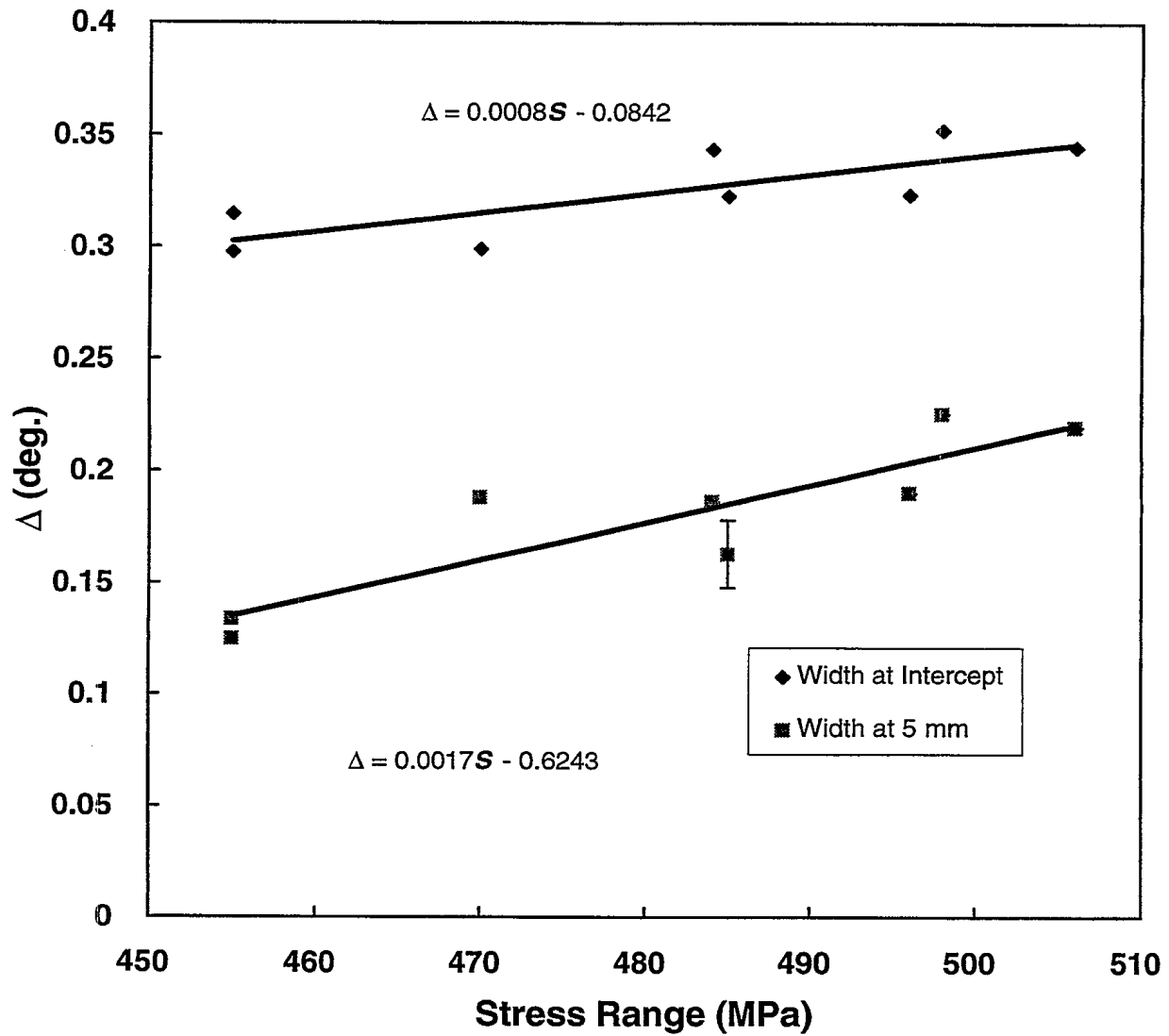
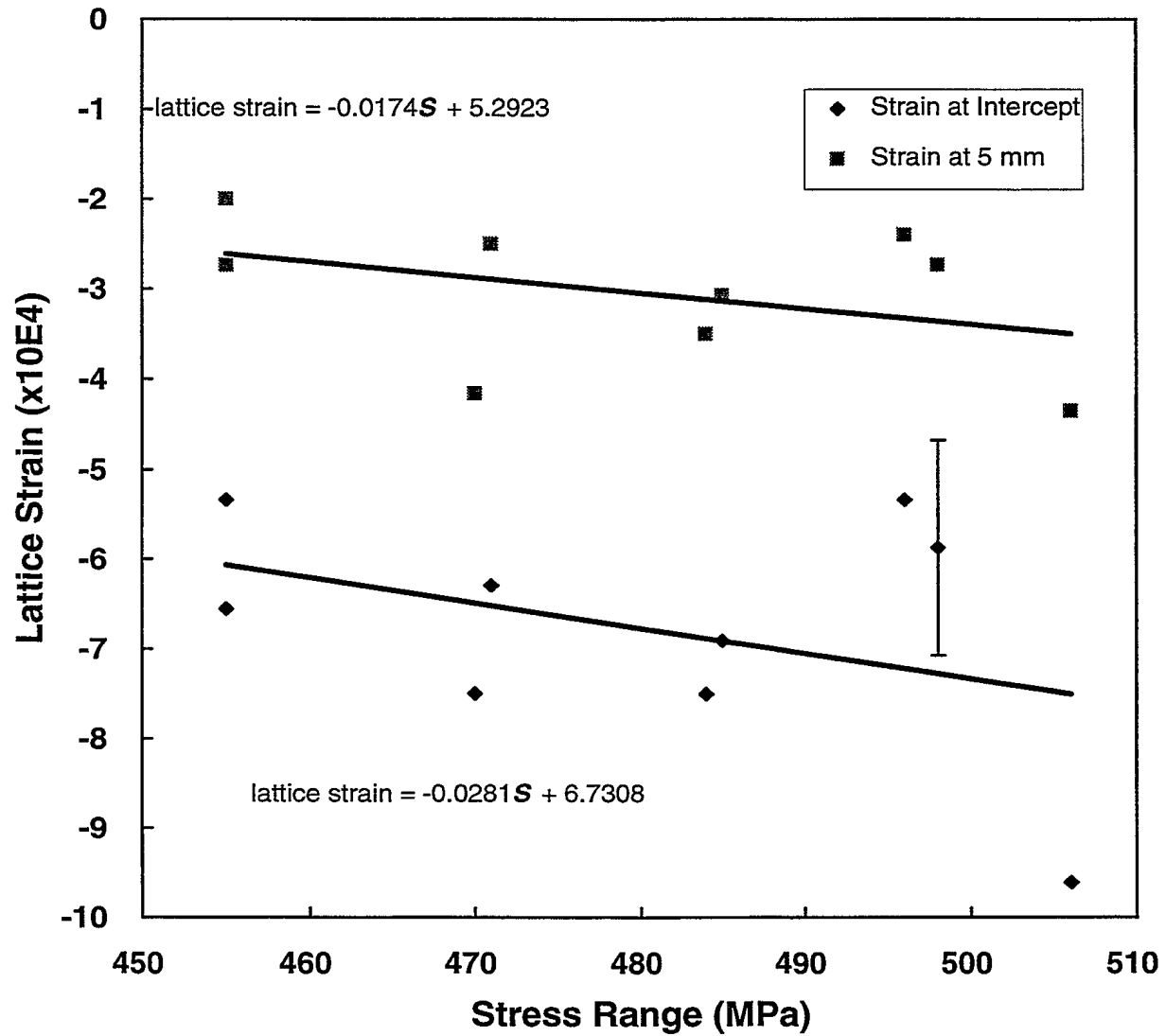
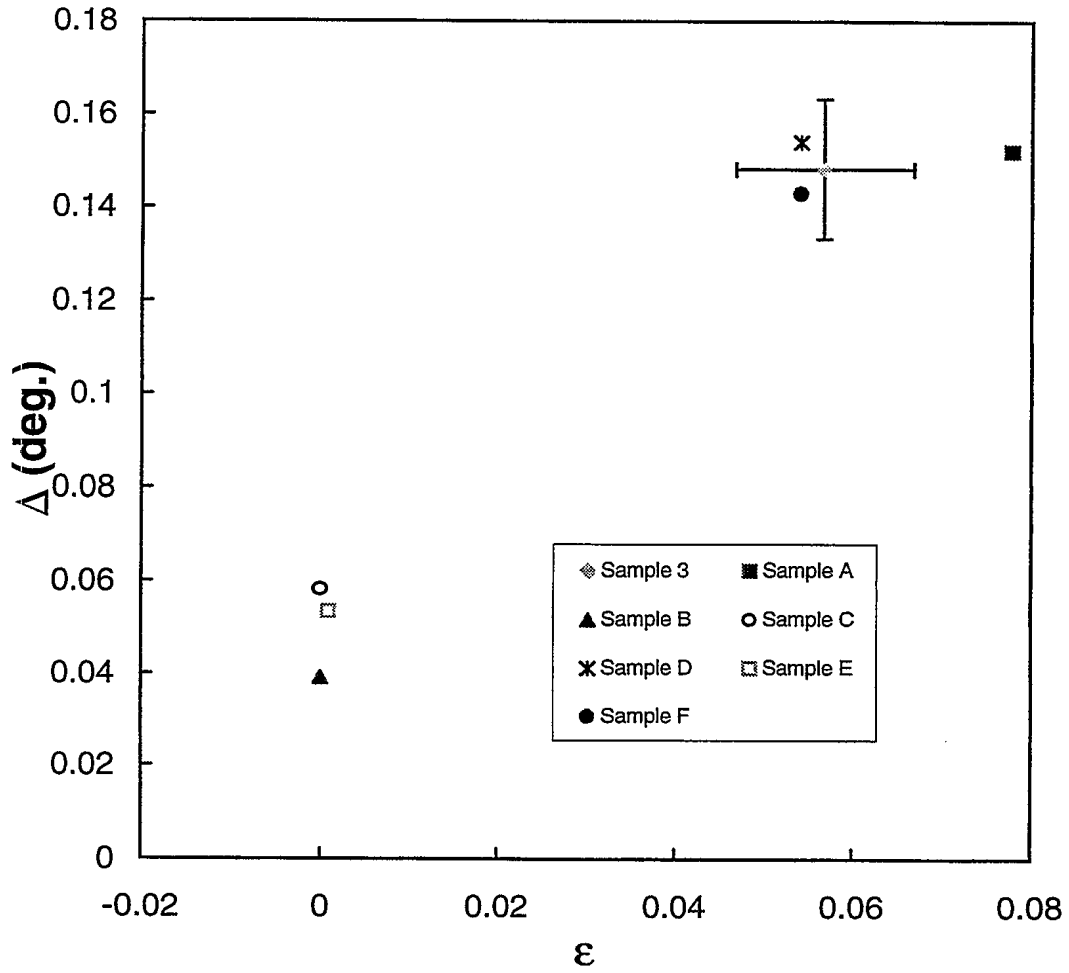


Figure 3 The diffraction linewidth at the break and 5mm away from the break as a function of fatigue stress range for nine samples cycled to failure.



**Figure 4** The residual lattice strain at the break and 5mm away from the break as a function of fatigue stress range for nine samples cycled to failure.



**Figure 5** The diffraction linewidth at the waist as a function of true macro-strain for seven unbroken samples.

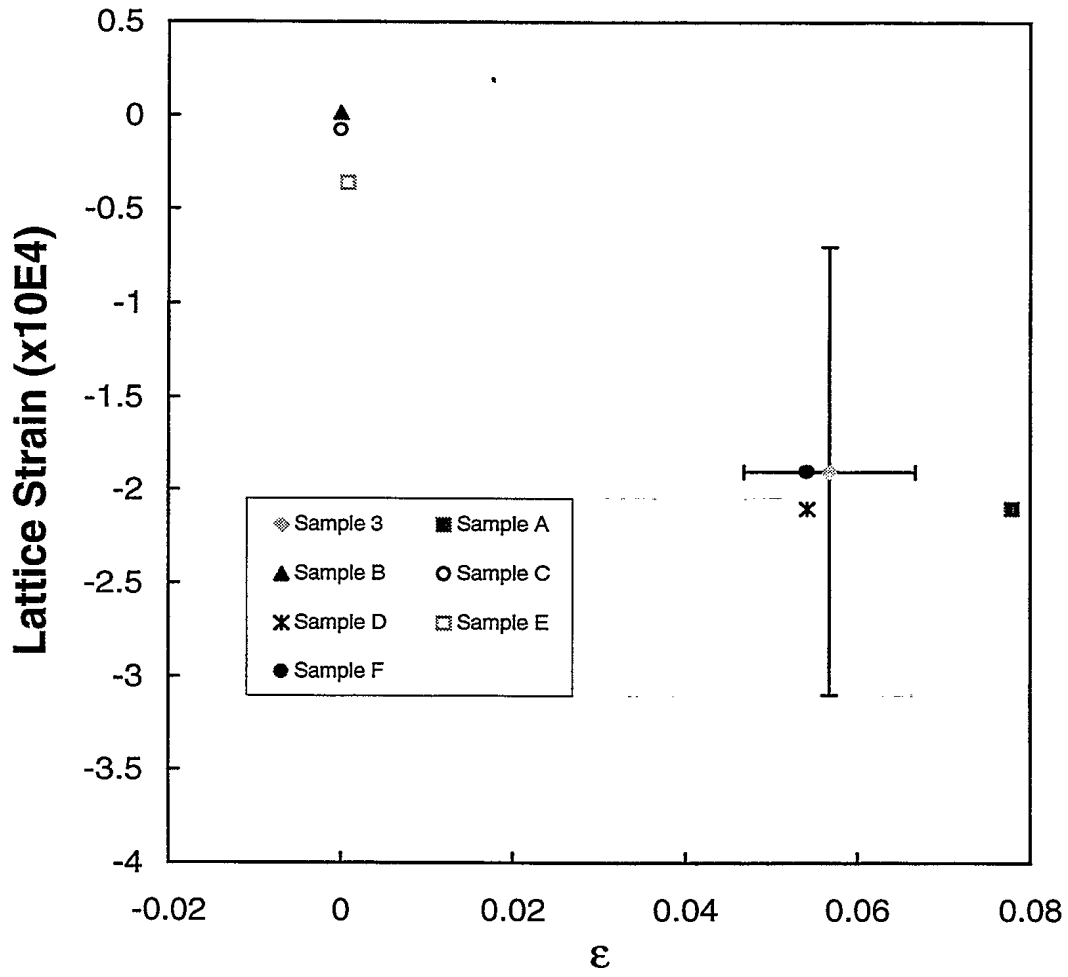


**Figure 6** The residual lattice strain at the waist as a function of true macro-strain for seven unbroken samples.

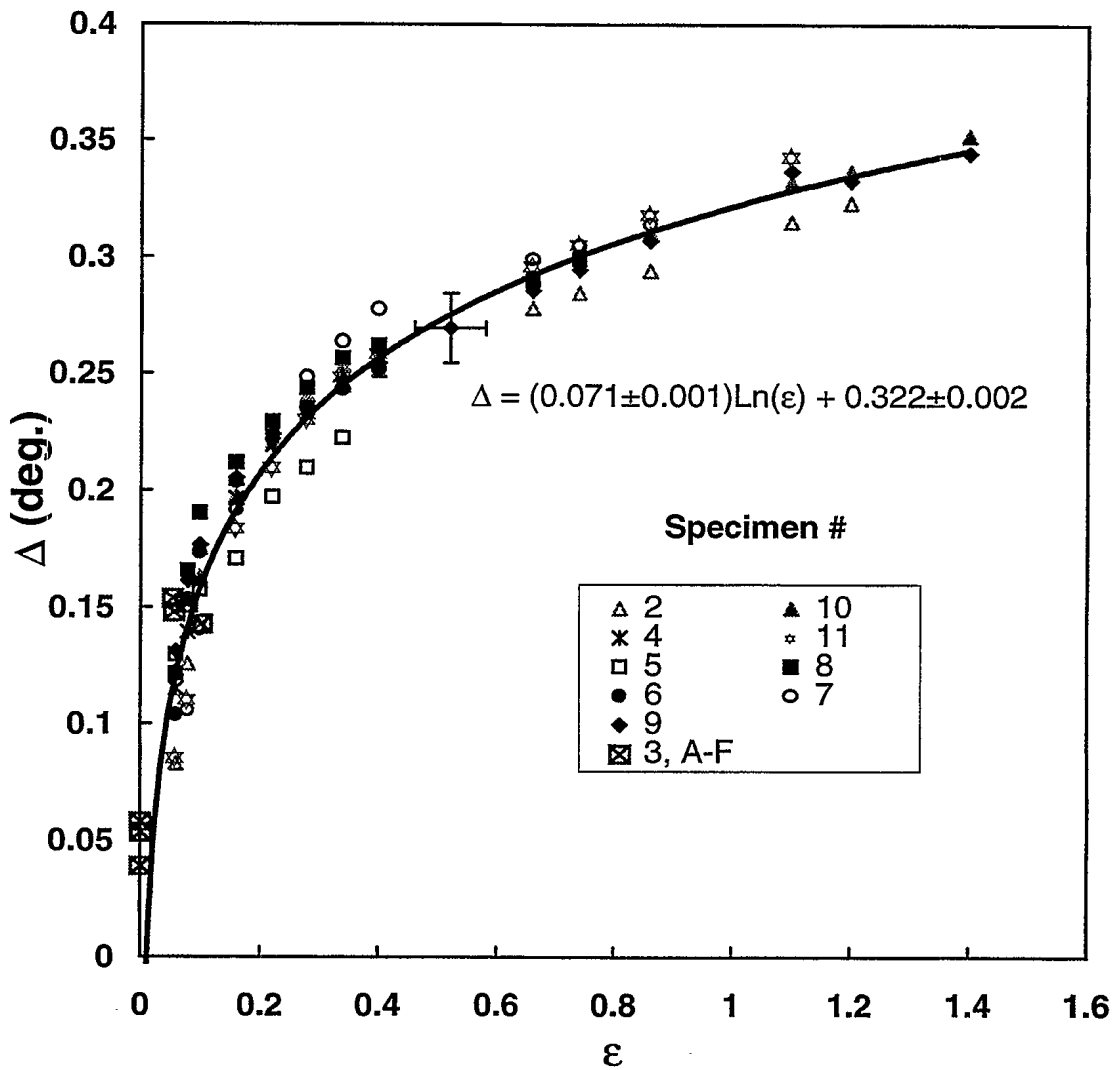


Figure 7 The (110) diffraction linewidth corrected for instrumental broadening as a function of true macro-strain for nine samples cycled to failure and seven unbroken samples.



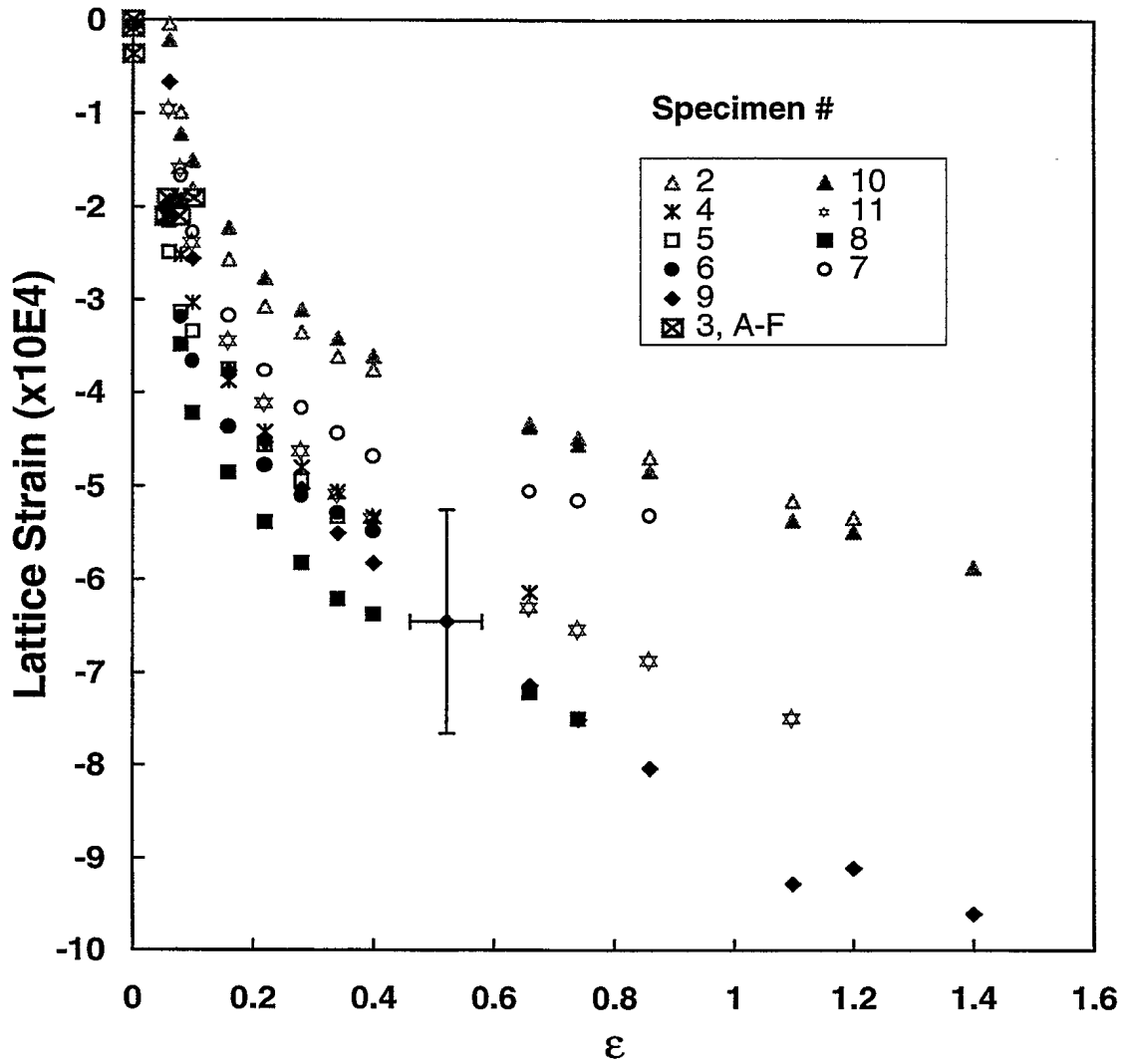
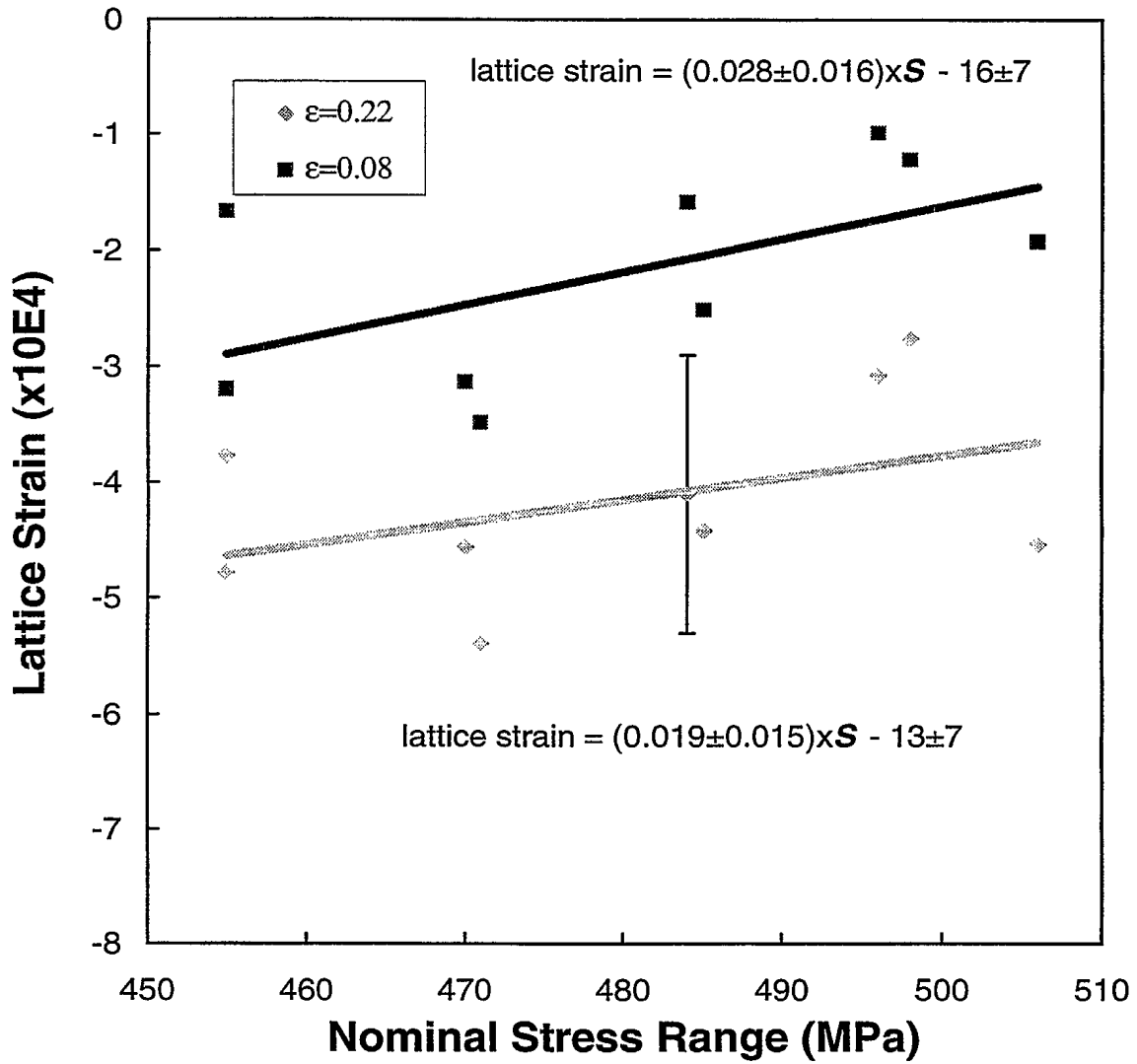


Figure 8 The residual lattice strain as a function of true macro-strain for nine samples cycled to failure and seven unbroken samples.



**Figure 9** The residual lattice strain as a function of fatigue stress range at two constant strain values for nine samples cycled to failure.